Surface-Anisotropic Polystyrene Spheres by Electroless Deposition

2 AUTHORS, INCLUDING:

Ilona Kretzschmar
City College of New York

93 PUBLICATIONS   **2,206** CITATIONS

Surface-Anisotropic Polystyrene Spheres by Electroless Deposition

Jing-Qin Cui and Ilona Kretzschmar*

*Chemical Engineering Department, Steinman Hall, The City College of New York,
140th St. and Convent Ave., New York, New York 10031*

Received June 16, 2006. In Final Form: August 8, 2006

Surfaces of sulfate-terminated polystyrene microspheres are anisotropically modified with silver nanoparticles covering 20–50% of the sphere surface using electroless deposition. A PDMS templating method is employed. Silver nanoparticles are found to deposit uniformly onto the exposed sphere surfaces. The deposition is diffusion-controlled and the nanoparticles adhere strongly to the polystyrene particles despite extensive exposure to ultrasonication. Silver content is confirmed by EDAX analysis. The final silver coverage is controlled via the PDMS pre-curing conditions.

Introduction

Surface-anisotropic particles are a new class of materials with interesting properties. They can, for example, exhibit amphiphilic character[1] and giant dipole moments,[2] act as templates for metal half-shells[3] and optical nanoprobes,[4] and show directional reactivity.[5]

Current partial surface modification methods[6–9] include, for example, vapor deposition,[3,7,10] stamping,[11] and functional group aided reactivity.[12,13] More recently, attention has turned toward electrochemical methods for particle surface modification.[8,14] The autocatalytic electroless deposition (ELD) of metal based on a reduction–oxidation reaction is important for the metallization of nonconducting surfaces.[15] ELD is highly selective, requires mild processing conditions, and works with low-cost equipment.[16] However, ELD is a liquid-phase technique, and the in situ particle growth occurs controllably, but homogeneously, on all surfaces exposed to the reaction solution. Thus, a templating mask is required for site-specific modification of surfaces.[6,8]

Results and Discussion

Our report describes a templating procedure that yields surface-anisotropic, silver-capped microspheres by electroless deposition of silver nanoparticles onto the exposed sphere surface. A schematic representation of the process is shown in Figure 1.
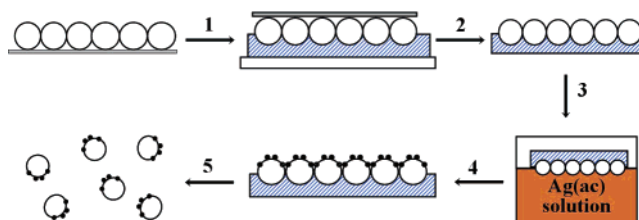

Figure 1. Cross sectional presentation of synthetic route to surface-anisotropic sulfate-terminated polystyrene (sPS) spheres. Silicon wafer (gray area); sPS spheres ($\bigcirc$); PDMS mask (blue hatched area); electrochemical solution (Ag(ac) solution); and silver nanoparticle ($\bullet$).

In brief, a monolayer of sulfate-terminated polystyrene (sPS) spheres is assembled on a silicon wafer and subsequently pressed into a pre-cured poly(dimethylsiloxane) (PDMS) mask. The PDMS mask with the partially embedded spheres, hereafter called sphere/PDMS composite, is pealed off the wafer after complete curing of the PDMS. The sphere/PDMS composite is then exposed to a silver salt solution, which results in deposition of silver nanoparticles on the exposed, negatively charged surfaces upon addition of ammonia and formaldehyde. Next, the silver-capped spheres are removed from the PDMS mask and re-dispersed into solution.

An ordered, closely packed monolayer is obtained via continuous convective assembly of sPS spheres on a silicon wafer using a simple cylindrical Teflon cell.[17–19] The cell employed for assembly consists of a Teflon ring of 1-cm inner diameter, a piece of silicon (110) wafer with a native oxide surface (University Wafer), and three paper clips to clamp the assembly together. The silicon wafer is used as obtained after cleaning in a high-pressure nitrogen flow. A total of 143 μL of a polystyrene sphere dispersion (2.4 $\pm$ 0.14 μm, Interfacial Dynamics Corporation) with a concentration of 1.1×10^8 spheres/mL is added to the cell covering the accessible area of the silicon wafer encircled by the Teflon ring. Samples are placed horizontally in a desiccator, which is kept in an oven at 40 °C for usually 6–8 h until all of the solvent has evaporated.

Figure 2a shows a variable-pressure scanning electron microscope (vp-SEM)[20] image of a monolayer of 2.4 μm sPS spheres obtained with an EVO40 Zeiss vp-SEM. The sPS spheres

* Corresponding author. E-mail: kretzschmar@ccny.cuny.edu.

(1) Glaser, N.; Adams, D. J.; Boker, A.; Krausch, G. *Langmuir* **2006**, *22*, 5227–5229.

(2) Takei, H.; Shimizu, N. *Langmuir* **1997**, *13*, 1865–1868.

(3) Love, J. C.; Gates, B. D.; Wolfe, D. B.; Paul, K. E.; Whitesides, G. M. *Nano Lett.* **2002**, *2*, 891–894.

(4) Behrend, C. J.; Anker, J. N.; McNaughton, B. H.; Brasuel, M.; Philbert, M. A.; Kopelman, R. *J. Phys. Chem. B* **2004**, *108*, 10408–10414.

(5) Snyder, C. E.; Yake, A. M.; Feick, J. D.; Velegol, D. *Langmuir* **2005**, *21*, 4813–4815.

(6) Perro, A.; Reculusa, S.; Ravaine, S.; Bourgeat-Lami, E. B.; Duguet, E. *J. Mater. Chem.* **2005**, *15*, 3745–3760.

(7) Paunov, V. N.; Cayre, O. *J. Adv. Mater.* **2004**, *16*, 788–791.

(8) Charnay, C.; Lee, A.; Man, S.-Q.; Moran, C. E.; Radloff, C.; Bradley, R. K.; Halas, N. J. *J. Phys. Chem. B* **2003**, *107*, 7327–7333.

(9) Nagle, L.; Ryan, D.; Cobbe, S.; Fitzmaurice, D. *Nano Lett.* **2003**, *3*, 51–53.

(10) Correa-Duarte, M. A.; Salgueiriño-Maceira, V.; Rodríguez-González, B.; Liz-Marzán, L. M.; Kosiorek, A.; Kandulski, W.; Giersing, M. *Adv. Mater.* **2005**, *17*, 2014–2018.

(11) Cayre, O.; Paunov, V. N.; Velev, O. D. *J. Mater. Chem.* **2003**, *13*, 2445–2450.

(12) Fujimoto, K.; Nakahama, K.; Shidara, M.; Kawaguchi, H. *Langmuir* **1999**, *15*, 4630–4635.

(13) Petit, L.; Sellier, E.; Duguet, E.; Ravaine, S.; Mingotaud, C. *J. Mater. Chem.* **2000**, *10*, 253–254.

(14) Jackson, J. B.; Halas, N. J. *J. Phys. Chem. B* **2004**, *105*, 2743–2746.

(15) Rickerby, J.; Steinke, J. H. G. *Chem. Rev.* **2002**, *102*, 1525–1550.

(16) Mallory, G. O.; Hajdu, J. B. *Electroless Plating – Fundamentals and Application*; William Andrew Publishing: Norwich, 1990.

(17) Dimitrov, A. S.; Nagayama, K. *Langmuir* **1996**, *12*, 1303–1311.

(18) Denkov, N. D.; Velev, O. D.; Kralchevsky, P. A.; Ivanov, I. B.; Yoshimura, H.; Nagayama, K. *Langmuir* **1992**, *8*, 3183–3190.

(19) Silvera-Batista, C. A.; Kretzschmar, I. *Junior Scientist Conference '06*; Vienna University of Technology: Vienna, 2006.

(20) Erickson, B. *Anal. Chem.* **1997**, 7499A-752A.

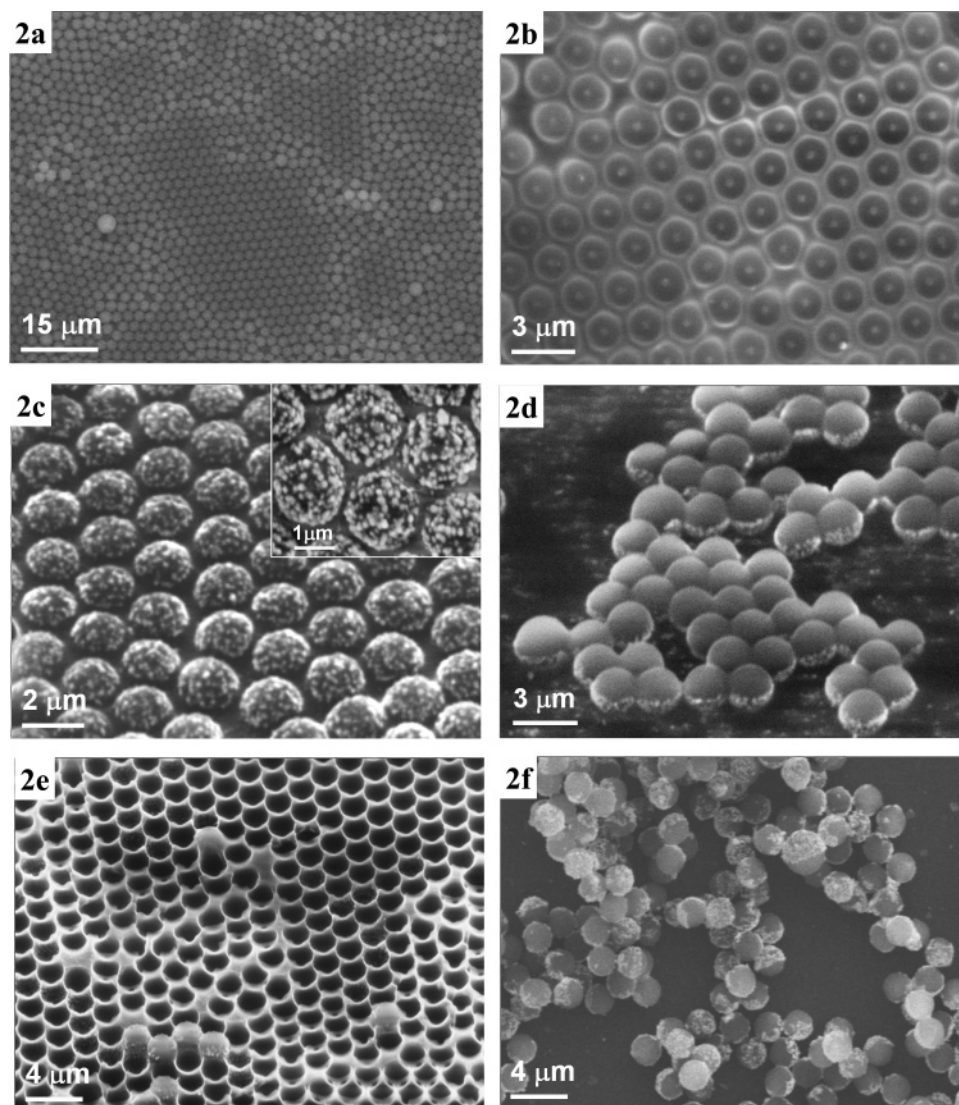**Figure 2.** Scanning electron microscopy (SEM) images of 2.4 μm sPS spheres. (a) sPS sphere monolayer on silicon wafer with native oxide. Scale bar: 15 μm. (b) sPS spheres embedded in PDMS mask. Scale bar: 3 μm. (c) sPS spheres after electroless silver deposition, 45° tilted. Scale bar: 2 μm. Inset: High-resolution image of silver deposit (AgNP) showing nanoparticles with 50−150 nm diameters. Average AgNP number per sphere is 75 ± 15. Scale bar: 1 μm. (d) Silver modified sPS spheres on double-sided adhesive carbon tape (55° tilt). White spots visible at the bottom of spheres are AgNPs. Scale bar: 3 μm. (e) Empty PDMS mask with spherical impressions from sPS spheres at 45° tilt. A few spheres are left behind in the PDMS mask. Scale bar: 4 μm. (f) Surface-anisotropic 2.4 μm silver-modified sPS spheres released from the sphere/PDMS composite (see text). Scale bar: 4 μm.

assemble into a monolayer showing domains of close packing. The monolayer also exhibits regions of square-lattice packing and contains defects such as domain boundaries and local disorder caused by variations in particle size.

In contrast to the disperse sphere patterns observed by Paunov[7] and Aveyard[21,22] for the colloidal assembly of like-charged spheres at the oil−water interface, the negatively charged sPS spheres (charge content listed by manufacturer: 20 μEq/g) form close-packed monolayers despite the electrostatic repulsion during convective assembly on the silicon wafer. This observation can be rationalized by the action of immersion capillary forces between the particles during evaporation. The immersion force is strongly dependent on the wetting properties of the particles (i.e., position of the contact line and magnitude of the contact angle). As the solvent evaporates, the film in which the particles are trapped becomes thinner and the deformation of the liquid surface increases resulting in a stronger capillary interaction between the particles. In contrast, the electrostatic repulsion force between the like-charged particles decreases, as the particles are wetted less enabling the immersion capillary force to overcome the electrostatic repulsion.[23]

The average domain size is about 20 × 40 μm^2 containing approximately 150 close-packed spheres. It is possible to prepare larger areas of close packing by optimizing assembly temperature and humidity, suspension volume, particle volume fraction, sphere diameter, and Teflon cell dimensions.[17,19] The sPS spheres are successfully embedded in the PDMS mask such that part of their surface stays exposed and are subsequently removed from the silicon wafer. Curing of PDMS occurs by a temperature-dependent organo-metallic cross-linking reaction.[24] The stiffness of the PDMS mask can be varied by pre-curing at elevated temperatures

(21) Aveyard, R.; Clint, J. H.; Nees, D.; Paunov, V. N. *Langmuir* **2000**, *16*, 1969−1979.
(22) Aveyard, R.; Binks, B. P.; Clint, J. H.; Fletcher, P. D. I.; Horozov, T. S.; Neumann, B.; Paunov, V. N.; Annesley, J.; Botchway, S. W.; Nees, D.; Parker, A. W.; Ward, A. D.; Burgess, A. N. *Phys. Rev. Lett.* **2002**, *88*, 246102.

(23) Kralchevsky, P. A.; Nagayama, K. *Adv. Colloid Interface Sci.* **2000**, *85*, 145−192.
(24) Campbell, D. J.; Beckman, K. J.; Calderon, C. E.; Doolan, P. W.; Ottosen, R. M.; Ellis, A. B.; Lisensky, G. C. *J. Chem. Educ.* **1999**, *76*, 537−541.

for different time intervals and enables the control of the sPS sphere embedment depth (see below). The PDMS mask is pre-cured for ∼10 min at 70 °C in an oven followed by addition of the monolayer sample (Figure 1, step 1). Then the PDMS−spheres−wafer sandwich structure is cured for another 2 h at 70 °C. After curing, the PDMS mask is peeled off the silicon wafer, simultaneously removing the monolayer of spheres (Figure 1, step 2). Figure 2b shows an SEM image for the sphere/PDMS composite with the spheres appearing partially embedded in the mask. The approximately 0.2 μm gaps between neighboring spheres and the smaller average size of the spheres compared to their original size (1.8 ± 0.1 μm vs 2.4 ± 0.1 μm) indicate more than 50% embedment. An embedment depth of 2.0 ± 0.1 μm is determined using the actual sphere size and the exposed area shown in Figure 2b. Interestingly, some spheres have assumed a polygonal shape in contrast to their spherical shape exhibited in the monolayer (Figure 2a). Possible reasons for the sphere deformation are the force acting during PDMS mask stamping combined with the close packing of the initial monolayer and the non-cross-linked, soft nature of the sPS spheres (T_g = 100 °C).[25] The white rings observed around some of the spheres are likely the result of residual charging caused by the electron beam scanning the sample, while the white points at the center of each sphere indicate where the spheres have been in contact with the silicon wafer.

The partial embedment of the sPS spheres enables us to modify the exposed surface area using silver electroless deposition. The sphere/PDMS composite is placed upside down on 0.50 mL of a 0.003 M silver acetate (AgCH$_3$COO; Ag(ac); 99%, Sigma-Aldrich) aqueous solution such that the side with the exposed spheres is in contact with the solution (Figure 1, step 3) and is kept in the dark for 4 h at room temperature to facilitate Ag$^+$−SO$_4^-$ association. Note PDMS floats on the reaction solution due to its lower density (0.84 g/cm^3). Next, 0.08 mL of 1.0 N aqueous ammonium hydroxide (NH$_3$ · H$_2$O, Acros Organics) is added to the reaction mixture. The solution is stirred at 95 rpm for 5 min. Then 0.04 mL of an aqueous 12% formaldehyde solution (diluted from 20% HCHO, Tousimis Research Corpora-tion) is added to the stirred mixture at room temperature and stirred until completion of the deposition reaction indicated by a change in color of the solution from transparent to yellowish brown. The sample is taken out of the solution after the reaction and rinsed thoroughly with deionized (DI) water (Figure 1, step 4) and left to dry at room temperature. Successful silver deposition onto the spheres is accompanied by a change in color of the sample from whitish to yellowish-brown. The yellowish-brown color does not fade during rinsing with DI water.

Silver sphere/PDMS composites are imaged with SEM and reveal silver cluster formation on the exposed sPS sphere surfaces. Figure 2c presents an exemplary SEM image of the sphere/PDMS composite after silver deposition at 45° tilt. Comparison of the image in Figure 2c to that depicted in Figure 2b shows that most of the spheres stay embedded in the PDMS despite exposure to the reaction solution and agitation of the sample by stirring. The main difference between panels b and c in Figure 2 is that there are close-packed, circular areas with white spots visible after electroless deposition in Figure 2c, which coincide with the positions of the exposed sPS sphere surfaces in the PDMS mask in Figure 2b. High-resolution SEM imaging of the white spots (Figure 2c, inset) reveals particles with diameters ranging from 50 to 150 nm. This result is in good agreement with the observation by Mayer et al. that silver nanoparticles form on

the surface of carboxylated polystyrene spheres when exposed to silver acetate and formaldehyde.[26] Energy-dispersive X-ray analysis identifies the white deposit as silver (see the Supporting Information).

The silver nanoparticles (AgNPs) form uniformly on all exposed sPS sphere surfaces but exhibit random patterns. Silver particle formation and agglomeration are also observed in the reaction solution, whereas deposition of silver on the PDMS mask is negligible. According to the manufacturer, the spheres have a surface charge density of 8.1 μC/cm^2 equivalent to 9.1 × 10^6 SO$_4^-$ groups per sphere. Using the embedment depth of 2.0 ± 0.1 μm, we calculate the number of SO$_4^-$ groups on the exposed surface as 1.55 × 10^6. This number is much larger than the average number of 75 ± 15 silver nanoparticles (d_{AgNP} ∼ 150 nm) found on each exposed sphere surface corresponding to ∼55% coverage (Figure 2c, inset). The rationale for this observation is that formaldehyde is a slow reducing agent[26] giving rise to the formation of only a few nucleation sites. The sulfate groups act as binding sites for Ag$^+$ ions, which are subsequently reduced to elemental silver. The elemental silver starts the autocatalytic reaction acting as surface nucleation site facilitating further silver reduction and AgNP growth.[26] The electroless deposition process is either controlled by the rate of diffusion of the reactants to the reacting surface (diffusion controlled) or by the rate of an electrochemical reaction step (kinetically controlled). Our preliminary study of the effect of stirring rate on the deposit morphology shows that the slower stirring rates give sparser and smaller silver nanoparticles, whereas higher stirring rates result in a denser deposit and more agglomeration (unpublished data).[27] The results suggest that the silver deposition process is diffusion controlled.

Sonication is utilized to test the stability of the nanoparticles and their adhesion to the sphere surface. The AgNP-sphere/PDMS samples are exposed to ultrasonication for 50 min at a frequency of 40 kHz (Bransonic Ultrasonic Cleaner 1510) in an aqueous solution. No apparent loss of the Ag deposit is observed. The silver particles adhere strongly to the sPS spheres and the spheres also stay embedded in the PDMS mask. There are a couple of spheres that appear rotated or out of position revealing the partial silver deposit on their surfaces (data not shown). These observations allow the conclusion that AgNPs are formed at and adhere to the sPS sphere surface, but do not elucidate whether the silver particles prefer to accumulate in solution or on the sPS sphere surface under the reaction conditions employed.

The silver-modified spheres are removed from the PDMS mask using a double-sided adhesive carbon tape. The carbon tape (Structure Probe INC.) is mounted onto a silicon wafer. Then the AgNP-sphere/PDMS composite is pressed onto the carbon tape. The PDMS mask is carefully peeled off and most spheres are removed from the PDMS mask while keeping their close-packed pattern. The backside of the spheres is imaged in Figure 2d. In contrast to the frontside shown in Figure 2c, the majority of the exposed sphere surfaces looks smooth and shows no sign of silver deposition with the exception of a thin stripe of white spots on the bottom periphery of the spheres visible because the sample is tilted by 55°. Figure 2d also shows AgNPs on the carbon tape without sPS spheres; most likely resulting from disruption of the AgNPs/sPS sphere coordination. Figure 2e shows the empty PDMS mask after removal of the spheres. A few spheres stay trapped in the PDMS mask.

To re-disperse the silver-modified sPS spheres (Figure 1, step 5), the sphere/PDMS composite is stretched and the AgNP-

(25) Brandrup, J.; Immergut, E. H. *Polymer Handbook*; John Wiley & Sons: New York, 1989.

(26) Mayer, A. B. R.; Grebner, W.; Wannemacher, R. *J. Phys. Chem. B* **2000**, *104*, 7278−7285.

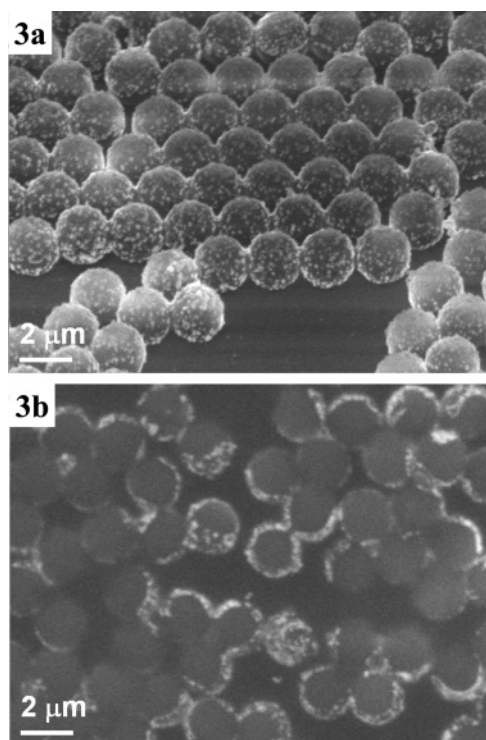(27) Cui, J.-Q.; Kretzschmar, I. Unpublished results.

Figure 3. (a) SEM image of silver-modified sPS sphere/PDMS composite with less embedded spheres and tilted by 45°. Scale bar: 2 μm. (b) SEM image of silver-modified 2.4 μm sPS spheres removed from PDMS mask with a double-sided adhesive carbon tape. Scale bar: 2 μm.

spheres are scratched from the PDMS mask with a metal blade according to the method reported by Paunov et al.[7] A white residue is found on the blade's edge after the procedure. A water droplet is spread on a piece of silicon wafer and the blade is dipped into it dissolving the white residue. The sample is left to dry in air and examined with SEM. Figure 2f shows an exemplary SEM image of an area with spheres on the dried sample. Large agglomerates with random orientation of surface-anisotropic spheres are found at the rim of the dried droplet. The silver modification appears unchanged by the blade collection process on most of the spheres.

Variation of the pre-curing time controls the area modified with AgNPs on the sPS spheres. The diameters of the circular areas with the AgNP particles in the PDMS mask shown in Figure 2c are measured as $1.8 \pm 0.1 \mu$m. Based on the Pythagorean theorem, the height of the modified sPS sphere surface is calculated as 0.41 μm representing approximately 20% of the entire sPS sphere surface. Extending the PDMS pre-curing time by approximately 20% while keeping all other parameters constant leads to less deeply embedded sPS spheres. In the samples with longer pre-cured PDMS, a larger surface portion of the sPS spheres stays exposed leading to a bigger AgNP cap. Figure 3a shows the AgNP deposit on a 45°-tilted sample, for which the PDMS mask was pre-cured for a longer time. The backside view of the spheres after extraction from the PDMS mask with the carbon tape shows that more than 50% AgNP coverage is obtained (Figure 3b).

Conclusions

In conclusion, we have developed a protocol for a solid templating mask, which is employed for the electroless modification of sulfate-terminated polystyrene spheres with caps comprised of silver nanoparticles. The results for the 2.4 μm sPS spheres show that it is possible to prepare surface-anisotropic silver-capped sPS spheres via electroless deposition. Preliminary results suggest that the electroless deposition is diffusion-controlled.[27] Further, we have shown that it is possible to control the embedment depth of spheres in a PDMS mask by changing the pre-curing time for the PDMS mask. Hence, the coverage area of the silver deposition can be controlled. Further work is in progress testing the applicability of other metals such as Au, Pd, and Ni, for the preparation of surface-anisotropic microspheres using electroless deposition.

Supporting Information Available: EDAX spectra and corresponding SEM images. This material is available free of charge via the Internet at http://pubs.acs.org.

LA061742U